Special Interest Group Meeting on Thermal Issues
Laboratory for Machine Tools and Production Engineering (WZL) of
RWTH Aachen, Germany, February 2020
www.euspen.eu

Thermal modelling using dynamic mode decomposition for thermal error compensation in the temperature domain

Nemwel K. Ariaga[1], Andrew P. Longstaff[1], Simon Fletcher[1], Wencheng Pan[1], Naeem S. Mian[1]

[1]*Centre for Precision Technologies, University of Huddersfield,*

Nemwel.Ariaga@hud.ac.uk

Abstract
Thermal errors significantly impact the performance of precision machine tools. Compensation enables control of these errors in a flexible manner but depends on the prediction accuracy of models. Thermal error compensation is often performed in the displacement domain, but in certain applications can be done in the temperature domain using models that predict the thermal distribution. These predictions are used to regulate external heat sources such that the effects of thermal errors at the point of interest are controlled. In most instances, reduced order models for predicting thermal distribution are obtained from analytical tools such as finite element analysis (FEA). However, these methods require the boundary conditions to be well-defined, which may be suboptimal when the resulting model is applied under different sets of conditions such as a moving heat disturbance.
This paper explores the performance of Dynamic Mode Decomposition (DMD) for modelling thermal dynamics in a thin aluminium plate, representing a hot inkject printer head. DMD is an efficient, empirical, reduced-order modelling approach that obtains locally linear models of nonlinear dynamics. FEA simulation of a moving heat load is used to obtain modelling data. DMD is observed to extract and model low frequency dynamics associated with heat conduction and convection. The models produced have prediction residuals that fall within $\pm$ 0.25 ℃. This has potential application in implementation of a thermal error compensation controller.

Compensation; Decomposition method; Modelling; Thermal error

1. Introduction

Thermal errors significantly impact the performance of precision machine tools and account for 50-75% of the total geometric errors in workpieces [1, 2]. Compensation is a convenient approach for reducing these errors that can be implemented after build or installation of the machine tool. Research and commercial systems often compensate in the displacement (thermal error) domain. Models are used to predict the thermal deviation at the point of interest, as a function of running parameters (e.g. spindle use) or temperature measurements, which is then offset by physical actuation. Many different modelling approaches have been implemented, such as Artificial Neural Networks (ANNs)[3], Adaptive Neural Fuzzy Inference Systems (ANFIS) [4] and Finite Element Analysis (FEA) [[5]models.

Alternatively, the thermal error can be reduced in the temperature domain. This strategy uses external heat sources and sinks to control the temperature distribution within the structure such that the thermal displacement errors are reduced[6]–[8]. A particular advantage of this approach is in reducing the bending moments, and therefore angular deviations that can occur. This requires accurate models of the thermal distribution dynamics.

Reconstruction of the heat distribution requires spatial discretisation of the component being modelled, which results in large matrices that define the system properties. These matrices strain storage and computational resources needed for control and error compensation. Therefore, various model order reduction (MOR) approaches are used to obtain tractable models. These methods can be categorised into numerical-based MOR and empirical-based MOR methods.

Numerical-based MOR methods apply model reduction on the spatially discretised heat conduction equation based on Fourier's law of heat conduction. These methods include Balanced Truncation [6], Moment Matching [7] and Thermal Modal Analysis [8]. These have been applied in obtaining reduced order models for machine tool structures, rubber curing, hot inkjet printing and photolithography processes. Though numerical-based MOR methods are computationally efficient, the need for accurate definition of boundary conditions may decrease the optimality of the reduced order models under different thermal load conditions [9].

Empirical-based MOR methods depend on snapshot measurements of the thermal dynamics, which can be obtained from numerical simulations or experimentation. Unlike numerical-based MOR methods which produce models optimised for given boundary condition definitions, empirical-based MOR adapt to observed dynamics of the system. This is advantageous in many instances such as when the process being modelled is subjected to different loading conditions. Proper orthogonal decomposition (POD) is a widely used empirical dimensionality reduction technique. POD is used for finding reduced bases, the POD modes, which successively maximize the variance in the data. The obtained modes can be applied to selecting optimal sensor placement positions for reconstructing the thermal distribution for the given data [9]. However, the modelling effectiveness of POD reduces under different thermal loading dynamics because classical POD does not model how the modes evolve in time. Though extensions of POD, such as the POD-Galerkin, and the discrete empirical interpolation method (DEIM) enable modelling of dynamic systems [10], they can be unstable [11]. Dynamic Mode Decomposition (DMD) is an empirical MOR approach that models nonlinear dynamics using

a locally linear model obtained through Eigen decomposition [12]. DMD is closely related to the Koopman operator, which is a linear mapping of the states of a nonlinear system. DMD is widely used in extracting low dimensional patterns that govern complex high dimensional unsteady fluid flows [13]. The computational efficiency of DMD in extracting the reduced order state transition matrix of a dynamical system can be recursively applied to adapt to changes in the system dynamics. This is useful in cases such as changing loading conditions or changing boundary conditions. This present work explores the use of DMD as a MOR tool for compensation in the temperature domain.

The paper is organised as follows. First, the DMD algorithm is introduced in Section 2, then the simulation setup is described in Section 3. Modelling results and discussion are presented in Section 4. Finally, the conclusions are presented in Section 5.

2. Dynamic Mode Decomposition (DMD)

Fourier's law of heat conduction describes the heat conduction in a discretised structure as follows:

$$\boldsymbol{C}\dot{\boldsymbol{T}}(t) + \boldsymbol{K}\boldsymbol{T}(t) = \boldsymbol{q}(t) \tag{1}$$

Where $\boldsymbol{T}(t) \in \mathbb{R}^N$ is a vector of the temperature values of each element at time t, $\boldsymbol{C} \in \mathbb{R}^{N\times N}$ is the capacity matrix, $N$are the number of discrete elements in the structure, $\boldsymbol{K} \in \mathbb{R}^{N\times N}$ is the conductivity matrix and $\boldsymbol{q} \in \mathbb{R}^N$ represents the heat loads applied to each element.

The DMD algorithm finds an approximate locally linear model of the heat conduction dynamical system from sampled data [14]. This translates to finding the state transition matrix when the control input is not specified such that

$$\boldsymbol{x}_{k+1} = \boldsymbol{A}\,\boldsymbol{x}_k \quad \forall k = 1,2,\dots,m \tag{2}$$

Where the states $\boldsymbol{x}_k \in \mathbb{R}^N$ represent the temperature measurements of the elements/nodes at discrete time k and $\boldsymbol{A} \in \mathbb{R}^{N\times N}$ is the state transition matrix. $\boldsymbol{A}$ is computed to minimise the L2 norm such that

$$\arg\min_{\boldsymbol{A}} \|\boldsymbol{x}_{k+1} - \boldsymbol{A}\,\boldsymbol{x}_k\|_2 \quad \forall k = 1,2,\dots,m \tag{3}$$

The solution to this equation (2) is given by

$$\boldsymbol{x}_k = \sum_{j=1}^{N} \phi_j\, \lambda_j^k b_j = \boldsymbol{\Phi}\,\boldsymbol{\Lambda}^k \boldsymbol{b} \tag{4}$$

Where $\boldsymbol{\Phi} \in \mathbb{R}^{N\times N}$ consists of Eigen column vectors or modes of the transition matrix. $\boldsymbol{b} \in \mathbb{R}^N$ is a vector that scales the modes and represents the initial conditions that of the system such that $\boldsymbol{b} = \boldsymbol{\Phi}\boldsymbol{x}_1$. $\boldsymbol{\Lambda}^k$ is a diagonal matrix of Eigen values of $\boldsymbol{A}$ representing how the modes evolve at discrete time k. An equivalent continuous time evolution of the Eigen values can be obtained for systems that are sampled every Δt seconds by

$$\boldsymbol{\Lambda}^k = exp(\boldsymbol{\Omega} t), \;\; t = k \times \Delta t \tag{5}$$

In most applications it is not efficient to directly compute $\boldsymbol{A}$ because of the high dimension of the state vector. DMD takes advantage of the low dimensionality in the data using Singular Value Decomposition (SVD) to compute a low dimensional approximation of $\boldsymbol{A}$.

2.1. DMD algorithm

1. The state of the system is sampled to form m vectors which are combined to form two matrices

$$\boldsymbol{X} = \begin{bmatrix} | & | & & | \\ \boldsymbol{x}_1 & \boldsymbol{x}_2 & \dots & \boldsymbol{x}_{m-1} \\ | & | & & | \end{bmatrix} \tag{6}$$

$$\boldsymbol{X}' = \begin{bmatrix} | & | & & | \\ \boldsymbol{x}_2 & \boldsymbol{x}_3 & \dots & \boldsymbol{x}_m \\ | & | & & | \end{bmatrix} \tag{7}$$

Resulting in the discrete-time system equation

$$\boldsymbol{X}' = \boldsymbol{A}\,\boldsymbol{X} \tag{8}$$

Where $\boldsymbol{A}$= $\boldsymbol{X}'\,\boldsymbol{X}^{\dagger}$ and $\boldsymbol{X}^{\dagger}$ is the pseudoinverse of $\boldsymbol{X}$.

2. Obtain the SVD of $\boldsymbol{X}$

$$\boldsymbol{X} = \boldsymbol{U}\boldsymbol{\Sigma}\boldsymbol{V}^* \tag{9}$$

Where $U \in \mathbb{C}^{\boldsymbol{n}\times\boldsymbol{n}}$ are left singular vectors, $\boldsymbol{\Sigma} \in \mathbb{C}^{\boldsymbol{n}\times\boldsymbol{m}}$ are singular values and $\boldsymbol{V} \in \mathbb{C}^{\boldsymbol{m}\times\boldsymbol{m}}$ are right singular vectors.

3. Obtain a low dimensional representation of the data using the rank reduced SVD values

$$\boldsymbol{X} \approx \boldsymbol{U_r}\boldsymbol{\Sigma_r}\boldsymbol{V^*_r} \tag{10}$$

Where $r < m$, $\boldsymbol{U_r} \in \mathbb{C}^{\boldsymbol{n}\times\boldsymbol{r}}$, $\boldsymbol{\Sigma_r} \in \mathbb{C}^{\boldsymbol{n}\times\boldsymbol{r}}$ and $\boldsymbol{V_r} \in \mathbb{C}^{\boldsymbol{r}\times\boldsymbol{n}}$

4. Obtain the matrix $\boldsymbol{A} \in \mathbb{C}^{\boldsymbol{n}\times\boldsymbol{n}}$ using pseudoinverse of $\boldsymbol{X}$ i.e. $\boldsymbol{X}^{\dagger}$

$$\boldsymbol{A} = \boldsymbol{X}'\boldsymbol{X}^{\dagger} \approx \boldsymbol{X}'\boldsymbol{V_r}\boldsymbol{\Sigma_r}^{-1}\boldsymbol{U_r}^* \tag{11}$$

A low dimensional approximation of $\boldsymbol{A}$ is obtained by projecting $\boldsymbol{A}$ onto $\boldsymbol{U_r}$

$$\widetilde{\boldsymbol{A}} = \boldsymbol{U_r}^*\boldsymbol{A}\boldsymbol{U_r} = \boldsymbol{U_r}^*\boldsymbol{X}'\boldsymbol{V_r}\boldsymbol{\Sigma_r}^{-1} \tag{12}$$

Where $\widetilde{\boldsymbol{A}} \in \mathbb{C}^{r\times r}$

5. Compute the Eigen decomposition of $\widetilde{\boldsymbol{A}}$

$$\widetilde{\boldsymbol{A}}\boldsymbol{W} = \boldsymbol{W}\boldsymbol{\Lambda} \tag{13}$$

Where $\boldsymbol{W}$ are the Eigenvectors and $\boldsymbol{\Lambda}$ contains the Eigenvalues.

6. Finally, obtain the continuous time model of the system expressed in equations (4) and (5) by reconstructing the Eigenvalues and Eigenvectors of $\boldsymbol{A}$ (the DMD modes) using

$$\boldsymbol{\Phi} = \boldsymbol{X}'\boldsymbol{V_r}\boldsymbol{\Sigma_r}^{-1}\boldsymbol{W} \tag{14}$$

$$\boldsymbol{\Omega} = \boldsymbol{ln}(\boldsymbol{\Lambda})/\Delta t \tag{15}$$

$$\boldsymbol{b} = \boldsymbol{\Phi}^{\dagger}\boldsymbol{x}_1 \tag{16}$$

3. Methodology

The chosen problem represents a hot inkjet printing process or a photolithography process [8]. To replicate this example, FEA simulation of the transient thermal response of a thin aluminium

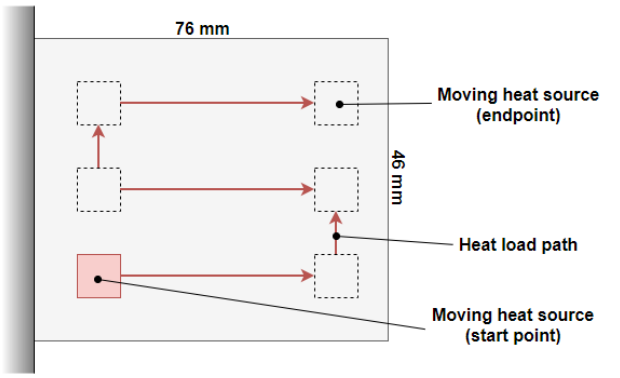

Figure 1. Moving heat load simulation setup

plate subjected to a moving heat load was run on ABAQUS CAE 2019 [15]. The simulation data was used in MATLAB R2019a to evaluate the performance of DMD in modelling the transient thermal dynamics. The aluminium plate of dimensions 76 mm x 46 mm x 0.1 mm was placed in contact with a moving heat source element of dimensions 2 mm x 2 mm x 0.1 mm as shown in Figure 1.

The body heat flux of the heat element was specified as $2\ W/\text{mm}^3$ over the contact surface of 2 mm x 2 mm. Extreme-ultraviolet lithography lasers have an intensity on the order of $4 \times 10^7\ W/\text{mm}^2$ [16]. The values of parameters used in the simulation are indicated in Table 1. Meshing of the aluminium plate resulted in 874 hexahedral elements (1,872 nodes). The heat source took 23 seconds to move from the start point to the end point with nodal temperature measurements recorded every 0.03125 seconds corresponding to 32 frames per second (fps). Modelling was then performed iteratively to obtain a proxy local linear model using data corresponding to 16 fps. At each iteration, the previous data over a defined time window was used for modelling and the resultant model used to make predictions of each node's temperature trajectory over the subsequent time window. The prediction accuracy of this data-driven model was then evaluated.

Table 1. Material property values and parameters used in simulation

Property	Value
Conductivity	$200\ mW/(mm\ ℃)$
Density	$2.7 \times 10^{-9}\ \text{ton/mm}^3$
Specific heat capacity	$900 \times 10^6\ \text{mJ/(ton ℃)}$
Moving heat load body heat flux	$2000\ mW/\text{mm}^3$
Convective heat transfer coefficient [5]	$0.006\ mW/(\text{mm}^2\ ℃)$
Environmental and initial temperature	20 ℃

4. Results and Discussion

The choice of the modelling window size is a function of the speed of the moving heat source. A small window would result in the model producing predictions with a lot of overshoots corresponding to the tangent of small dynamics in the data. On the other hand, a large window would reduce the model's ability to fit any dynamics within that window. In this work the modelling window was set at 3 seconds corresponding to 48 snapshots of data. The DMD models obtained iteratively using from the data were used to make on step ahead predictions at each node. A threshold of 11 leading singular values was used in rank reduction value while modelling. The root-mean-square error (RMSE) values of the predictions were plotted as shown in Figure 2. The RMSE values was observed to be highest along the path of the moving heat source. Two nodes were selected

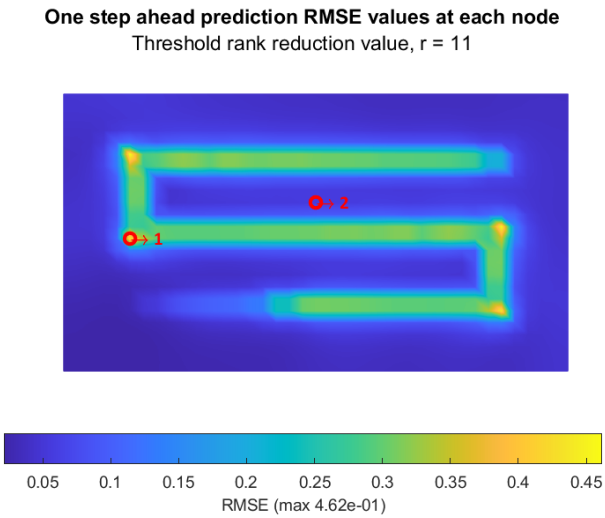

Figure 2. RMSE of one-step ahead prediction RMSE values

corresponding to the highest and lowest RMSE values and their predicted temperature trajectories plotted in Figure 3 and Figure 4 respectively.

Using 48 snapshots of data resulted in at most 48 nonzero singular values being obtained from the SVD, which represent the spectral content in the data. DMD is closely related to the Discrete Fourier Transform due to the use of SVD and Eigen decomposition [17]. The low frequency content is associated with heat conduction and convection, which are slow processes occurring over the entire window. On the other hand, the high frequency content results from external heating which is localised in space and time. DMD is observed to extract accurate models for predicting the low frequency content. This is observed in Figure 4 which is a plot of temperature predictions at a node where no point heating is applied. Residuals at this node falls within $\pm\ 0.2$ ℃. The predictive performance of DMD drops when modelling the high frequency data content. This is observed in Figure 3 where the residuals increase to $\pm\ 4$ ℃ as the heat source enters the region of the node. DMD assumes that spectral content lasts throughout the modelling and prediction time. This causes a drop in prediction accuracy for high frequency content which in this case have shorter

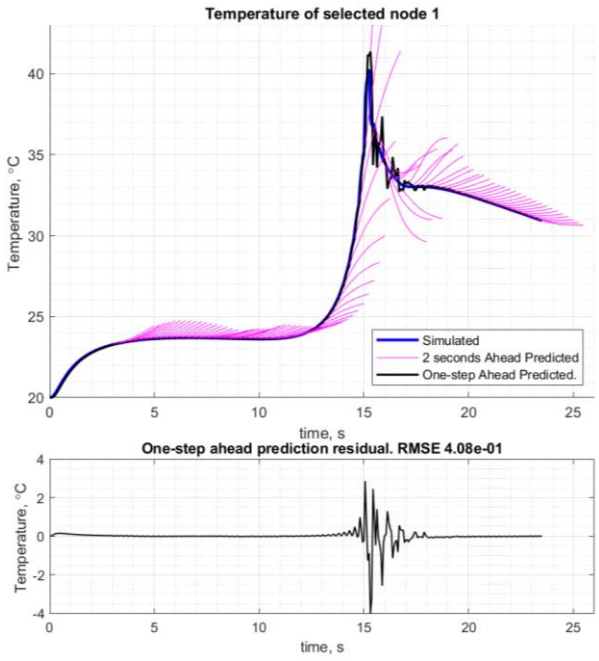

Figure 3. Predicted temperature trajectories and residual error at selected node 1

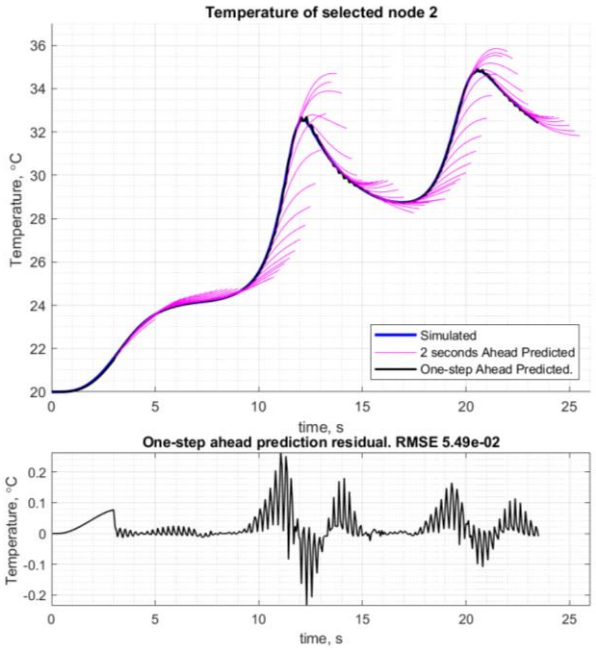

Figure 4. Predicted temperature trajectories and residual errors at selected node 2

durations. . This causes any inclusion of high frequency data to overshoot the actual values when used in prediction.

Determining what spectral content to retain is done by selecting the threshold point for rank reduction through soft or hard thresholding techniques [18]. However, these methods are adapted for models that reconstruct the data in the presence of noise as opposed to use in prediction of state trajectories. The hard threshold method suggests retaining the first 22 singular values which results in predictions with a maximum RMSE value of 5.41×10^{21}. This was found to be much higher than using lower rank truncation values of 5-11 as shown in Figure 2.

5. Conclusions

This paper has explored the use of dynamic mode decomposition (DMD) in modelling the thermal dynamics of a thin plate under the effects of a moving heat load. Simulation data was obtained from finite element analysis using ABAQUS CAE 2019 and used for modelling in MATLAB R2019a. The DMD algorithm was recursively applied on the data to obtain locally linear models at each time instance. The models were then used to obtain predictions of the temperature trajectories at each node.

The results obtained were observed to depend on tuning parameters that include the modelling window size and the rank reduction value used which determined the spectral content captured in the DMD models. The results indicate that DMD performs well in modelling the low frequency dynamics associated with heat conduction and convection with residuals of the prediction falling within $\pm$ 0.25 ℃. The residuals were observed to increase to slightly under $\pm$ 4 ℃ because of high frequency dynamics associated to heating by the moving heat source, particularly where the heat-source path changed direction rapidly. However, the increase in residuals were localised in both space and time which matched the position of the moving heat source. The overall performance indicates that DMD can be used to implement a thermal error compensation controller in the temperature domain.

Further work will take this principle to other problem domains, such as machine tool thermal modelling, where the sudden change in regime could be spindle speed, rather than location of the heat source.

The performance of DMD for application in thermal error compensation can be improved by developing a systematic method for selection of the tuning parameter that is suited for prediction. DMD can also be coupled with an optimal state estimator such as the Kalman filter to improve the performance under the effects of localised heating.

Acknowledgments

The authors gratefully acknowledge the UK's Engineering and Physical Sciences Research Council (EPSRC) funding of the Future Metrology Hub (Grant Ref: EP/P006930/1).

References

[1] M. Putz, C. Richter, and J. Regel, "Industrial relevance and causes of thermal issues in machine tools," Proc. Conf. Therm. Issues Mach. tools, no. June, pp. 127–139, 2018.

[2] J. Mayr et al., "Thermal issues in machine tools," CIRP Ann. - Manuf. Technol., vol. 61, no. 2, pp. 771–791, 2012.

[3] L. Ruijun, Y. Wenhua, H. H. Zhang, and Y. Qifan, "The thermal error optimization models for CNC machine tools," Int. J. Adv. Manuf. Technol., vol. 63, no. 9–12, pp. 1167–1176, 2012.

[4] A. M. Abdulshahed, A. P. Longstaff, S. Fletcher, and A. Myers, "Thermal error modelling of machine tools based on ANFIS with fuzzy c-means clustering using a thermal imaging camera," Appl. Math. Model., vol. 39, no. 7, pp. 1837–1852, 2015.

[5] N. S. Mian, S. Fletcher, A. P. Longstaff, and A. Myers, "Efficient estimation by FEA of machine tool distortion due to environmental temperature perturbations," Precis. Eng., vol. 37, no. 2, pp. 372–379, 2013.

[6] D. Oetinger and O. Sawodny, "Using model order reduction for disturbance feed forward control based on transient thermal finite element models," 2015 IEEE Conf. Control Appl. CCA 2015 - Proc., pp. 1486–1491, 2015.

[7] S. Bosselmann, T. Frank, M. Wielitzka, M. Dagen, and T. Ortmaier, "Thermal modeling and decentralized control of mold temperature for a vulcanization test bench," 1st Annu. IEEE Conf. Control Technol. Appl. CCTA 2017, vol. 2017-Janua, pp. 377–382, 2017.

[8] T. Morishima, R. Van Ostayen, J. Van Eijk, and R. H. M. Schmidt, "Thermal displacement error compensation in temperature domain," Precis. Eng., vol. 42, pp. 66–72, 2015.

[9] P. Benner, R. Herzog, N. Lang, I. Riedel, and J. Saak, "Comparison of model order reduction methods for optimal sensor placement for thermo-elastic models*," Eng. Optim., vol. 51, no. 3, pp. 465–483, 2019.

[10] C. Bikcora, S. Weiland, and W. M. J. Coene, "Reduced-order modeling of thermally induced deformations on reticles for extreme ultraviolet lithography," Proc. Am. Control Conf., pp. 5542–5549, 2013.

[11] M. Rathinam and L. R. Petzold, "A new look at proper orthogonal decomposition," SIAM J. Numer. Anal., vol. 41, no. 5, pp. 1893–1925, 2003.

[12] P. J. Schmid, "Application of the dynamic mode decomposition to experimental data," Exp. Fluids, vol. 50, no. 4, pp. 1123–1130, 2011.

[13] K. Taira et al., "Modal analysis of fluid flows: An overview," AIAA J., vol. 55, no. 12, pp. 4013–4041, 2017.

[14] J. H. Tu, C. W. Rowley, D. M. Luchtenburg, S. L. Brunton, and J. N. Kutz, "On dynamic mode decomposition: Theory and applications," J. Comput. Dyn., vol. 1, no. 2, pp. 391–421, 2014.

[15] D. Systèmes®, "Abaqus CAE - SIMULIATM." [Online]. Available: https://www.3ds.com/products-services/simulia/products/abaqus/abaquscae/. [Accessed: 17-Dec-2019].

[16] S. S. Harilal et al., "Spectral control of emissions from tin doped targets for extreme ultraviolet lithography," J. Phys. D. Appl. Phys., vol. 39, no. 3, pp. 484–487, 2006.

[17] C. W. Rowley, I. Mezi, S. Bagheri, P. Schlatter, and D. S. Henningson, "Spectral analysis of nonlinear flows," J. Fluid Mech., vol. 641, no. Rowley 2005, pp. 115–127, 2009.

[18] M. Gavish and D. L. Donoho, "The optimal hard threshold for singular values is 4/√3," IEEE Trans. Inf. Theory, vol. 60, no. 8, pp. 5040–5053, 2014.